



This is the accepted manuscript made available via CHORUS. The article has been published as:

Interlayer exciton complexes in bilayer math xmlns="http://www.w3.org/1998/Math/MathML">msub>mi>MoS/mi>mn>2/mn>/msub>/math>

Yanchong Zhao, Luojun Du, Shiqi Yang, Jinpeng Tian, Xiaomei Li, Cheng Shen, Jian Tang, Yanbang Chu, Kenji Watanabe, Takashi Taniguchi, Rong Yang, Dongxia Shi, Zhipei Sun, Yu Ye, Wei Yang, and Guangyu Zhang

Phys. Rev. B **105**, L041411 — Published 31 January 2022

DOI: 10.1103/PhysRevB.105.L041411

Interlayer exciton complexes in bilayer MoS_2

Yanchong Zhao[1,2], Luojun Du[3,*], Shiqi Yang[4,5], Jinpeng Tian[1,2], Xiaomei Li[1,2], Cheng Shen[1,2], Jian Tang[1,2], Yanbang Chu[1,2], Kenji Watanabe[6], Takashi Taniguchi[7], Rong Yang[1,8,9], Dongxia Shi[1,2,8], Zhipei Sun[3,10], Yu Ye[4,*], Wei Yang[1,2,9,*], Guangyu Zhang[1,2,8,9,*]

[1]Beijing National Laboratory for Condensed Matter Physics; Key Laboratory for Nanoscale Physics and Devices, Institute of Physics, Chinese Academy of Sciences, Beijing, 100190, China

[2]School of Physical Sciences, University of Chinese Academy of Science, Beijing 100190, China

[3]Department of Electronics and Nanoengineering, Aalto University, Tietotie 3, FI-02150, Finland

[4]State Key Laboratory for Mesoscopic Physics and Frontiers Science Center for Nano-optoelectronics, School of Physics, Peking University, Beijing 100871, China

[5]School of Physics and Academy for Advanced Interdisciplinary Studies, Peking University, Beijing 100871, China

[6]Research Center for Functional Materials, National Institute for Materials Science, 1-1 Namiki, Tsukuba 305-0044, Japan

[7]International Center for Materials Nanoarchitectonics, National Institute for Materials Science, 1-1 Namiki, Tsukuba 305-0044, Japan

[8]Beijing Key Laboratory for Nanomaterials and Nanodevices, Beijing 100190, China

[9]Songshan-Lake Materials Laboratory, Dongguan, Guangdong Province 523808, China

[10]QTF Centre of Excellence, Department of Applied Physics, Aalto University, FI-00076 Aalto, Finland

*Corresponding authors. Email: luojun.du@aalto.fi; ye_yu@pku.edu.cn; wei.yang@iphy.ac.cn; gyzhang@iphy.ac.cn

Atomically thin transition metal dichalcogenides can show a rich variety of bound exciton complex states, such as trions, biexcitons, Fermi polarons and phonon replicas, because of the reduced dielectric screening and enhanced Coulomb interaction. To date, the studies are mainly focused on the complexes of intralayer excitons, while the electrically tunable interlayer exciton complexes (IX complexes) remain elusive. Here we report the observation of IX complexes with large out-of-plane electric dipole, strong emission intensity and giant valley responses in bilayer MoS_2, through on-resonance photoluminescence spectroscopy. In sharp contrast to the small, positive circular dichroism of intralayer excitons, the circular polarization of IX complexes in bilayer MoS_2 can basically reach the theoretical limit (100%) but is negative. Such highly unusual light-valley responses of IX complexes in bilayer MoS_2 demonstrate the strongly suppressed valley depolarization and spin-preserving scattering of electrons during the formation. Remarkably, by breaking the time-reversal symmetry with an out-of-plane magnetic field, a record level of spontaneous valley polarization (7.7%/Tesla) is identified for IX complexes in bilayer MoS_2. The giant valley polarization of IX complexes in bilayer MoS_2, together with the feasibility of electrical/optical/magnetic control, provides a firm basis for the development of next-generation electronic and optoelectronic applications with valley functionalities.

In atomically thin transition metal dichalcogenides (TMDCs), the Coulomb interaction is strongly enhanced with respect to their bulk counterparts because of the largely reduced dielectric screening [1-3]. Consequently, apart from the conventional exciton comprising an electron and a hole, atomically thin TMDCs can show a rich variety of emergent exciton complex states [1], such as trions [4-8], biexcitons [9-14], Fermi polarons [15-17] and phonon replicas [18-21]. Understanding and controlling these exciton complexes are particularly important to fully utilize the potential of TMDCs for quantum photonic and optoelectronic applications. Although notable progress has been witnessed in the past few years, the studies are mainly focused on the complexes of intralayer excitons. Due to the absence of out-of-plane static electric dipole, intralayer exciton complexes cannot be tuned by the electric fields. In stark contrast, interlayer excitons (IXs) with spatially displaced wave-functions of electrons and holes are highly tunable with electric fields [22,23]. IXs, in principle, can also couple to other degrees of freedom to form the electric-field-tunable IX complexes for novel technological advances. Despite IXs have been demonstrated in a wide variety of TMDC homo- and hetero-structures [22,24-38], the IX complexes remain largely elusive.

In this work, we report the observation of IX complexes and their optical/magnetic addressability of valley pseudospin in bilayer MoS_2. Under the excitation of circularly polarized light near exciton resonance, we demonstrate that IX complexes in bilayer MoS_2 show a close-to-unity circular polarization, but with chirality opposite to the excitation photons. In addition, by breaking the valley degeneracy with an out-of-plane magnetic field, we observe a record level of spontaneous valley polarization (~ 7.7%/Tesla) for IX complexes in bilayer MoS_2. The giant valley

polarization of IX complexes in bilayer MoS_2 with both optical and magnetic addressability, together with the strong emission intensity and large out-of-plane electric dipole, provides a firm basis for the development of valley-functional electronic and optoelectronic applications.

High-quality, hexagonal boron nitride (*h*-BN) encapsulated bilayer MoS_2 devices with two symmetric graphene gates, as illustrated in Figure 1(a), are fabricated using the layer-by-layer dry transfer technique [39-41]. Three *h*-BN encapsulated bilayer MoS_2 devices (labeled as D1, D2 and D3) are studied and show consistent results. Unless otherwise specified, the data presented here are taken from device D1 in a high vacuum at 10 K. For device D1, the thicknesses of both top and bottom *h*-BN gate dielectrics are ~ 9.5 nm (Supplemental Material [42]). By applying the same (opposite) voltages on the two graphene gates, it varies the carrier density (out-of-plane electric field) in bilayer MoS_2 while keeping the electric field (doping) unchanged. Figures 1(c) and 1(d) present the color plot of photoluminescence (PL) spectra against electric field E_z under 532 nm off-resonance and 633 nm on-resonance excitations, respectively. Prominent IX emissions whose energies vary linearly with E_z, besides the well-known intralayer A excitons around 1.925 eV, can be unequivocally identified under both 532 nm (labeled as IX_{532}) and 633 nm excitations (dubbed as IX_{633}). Remarkably, in contrast to IXs in TMDC heterostructures with only one dipole moment, both IX_{532} and IX_{633} show two well-separated branches with opposite out-of-plane static electric dipole moments. This can be understood that because of the layer degeneracy of band structure, there are two IX species in bilayer MoS_2 [Figure 1(b)]: one with electron localized in lower layer and the other with electron resided in upper layer [30,43,44]. Via linear fitting [black dotted lines in Figures 1(c) and 1(d)], we extract the electric dipole moments of $\mu = \pm(0.56 \pm 0.01)\ e\ nm$ and $\mu = \pm(0.55 \pm 0.01)\ e\ nm$ for IX_{532} and IX_{633}, respectively, in good agreement with the value (e.g., $\pm 0.605\ e\ nm$) calculated based on hybridized hole wavefunctions (Supplemental Material [42]). For IX_{532}, the transition energy is ~ 1.995 eV at $E_z = 0$, about 70 meV above intralayer A excitons. The energy of IX_{532} matches perfectly the previous results, demonstrating that IX_{532} should belong to the same species as previously reported (that is, conventional spin-singlet IX comprising an electron and a hole with anti-parallel spin configuration) [30,31,38].

Figure 1f plots the transition energies against the applied electrical field for IX_{532} and IX_{633} extracted from Figures 1(c) and 1(d), respectively. Remarkably, IX_{633} are 40 meV smaller than IX_{532}, while the energies of intralayer A excitons excited by 633 nm radiation are exactly same with that under 532 nm excitation [Figure 1(e)]. This strongly indicates that IX_{633} observed under 633 nm on-resonance excitation should be a new species and different from the conventional species of IX_{532} which has been reported in previous work [30,38]. Further, compared to IX_{532}, the new species of IX_{633} exhibits unusual features. First, the energies of IX_{633} can be tuned from above the intralayer A exciton/trion to below the intralayer A exciton/trion (here we use trion to broadly refer to any quasiparticles formed by the interaction of exciton with a surrounding Fermi sea [4,15]), becoming the lowest excitonic state. This result is of particular importance because the lowest excitonic state usually plays a prominent role in the excitonic dynamics and applications [45].

Second, the peak width of IX_{633} (~ 7.5 meV) is much narrower than that of IX_{532} (~ 20.4 meV). This seems to indicate that IX_{633} have a long lifetime. Third, the quantum efficiency of IX_{633} are much larger than that of IX_{532} and can even be stronger than that of intralayer A excitons [Figure 1(e)]. Note that the quantum efficiency of A exciton under 633 nm on-resonance excitation is larger than that under 532 nm off-resonance excitation [46,47]. Fourth, the emission intensities of IX_{633} are highly tunable [Figure 1(g)]. When the energies of IX_{633} are tuned to the vicinity of intralayer A excitons or trions, the intensities of IX_{633} are strongly enhanced. Such highly unusual enhancement of emission intensities for IX_{633} may origin from the resonance energy transfer from intralayer A transitions or trions and deserves further in-depth studies to reveal the detailed microscopic mechanism [48].

To examine the origin of IX_{633}, we first perform the doping dependence of PL spectra to identify the possibility of IX trions. Figure 2(a) shows the color map of PL spectra against the doping density in the absence of electric field, excited by the 633 nm laser. Remarkably, IX_{633} follows the similar doping-driven intensity evolution of neutral intralayer A excitons, demonstrating its neutral nature. In addition, the energy spacing of 40 meV between IX_{633} and IX_{532} [Figure 1(f)], which is larger than the energy difference between intralayer A excitons and trions (~ 26 meV), also excludes the possibility that IX_{633} is trion species, since the binding energy of IXs should be smaller than that of intralayer excitons [28,30].

We then perform polarization-resolved magneto-PL, which can well identify the spin and valley indices of the constituent electrons and holes in the excitonic states [18,49-52], to further demystify origin of IX_{633}. Basically, there are two intrinsic IXs, i.e., spin-singlet and spin-triplet IXs. It is noteworthy that spin-triplet IXs in bilayer MoS_2 may also be optically bright because of the out-of-plane mirror symmetry breaking [53-56]. For spin-singlet and spin-triplet IXs, the valley Zeeman splitting defined as $\Delta E = E_{\sigma^+} - E_{\sigma^-}$ is $\Delta E_{\mathrm{spin-singlet}} = 2(\mu_l + \mu_v + \mu_c^t)B$ and $\Delta E_{\mathrm{spin-triplet}} = -2(\mu_l + \mu_s + \mu_v + \mu_c^b)B$, respectively, where μ_l is the intra-atomic d orbital magnetic moment of valence band, μ_s is the spin magnetic moment and $\mu_v/\mu_c^b/\mu_c^t$ denotes the valley orbital magnetic moments of valence/bottom conduction/top conduction bands (Supplemental Material [42]). Evidently, the valley Zeeman splitting of spin-singlet and spin-triplet IXs exhibits opposite signs and distinct magnitudes. Figure 2(b) shows the valley Zeeman splitting of IX_{633} and IX_{532}, together with that of intralayer A excitons. Strikingly, the valley Zeeman splitting of IX_{633} is exactly the same as that of IX_{532}, but has opposite sign to that of the intralayer A excitons. This indicates that the constituent electrons and holes in IX_{633} have the same spin and valley indices as that in IX_{532} [18]. In other words, IX_{633} also belongs to the neutral spin-singlet species. Considering the lower energy, IX_{633} should be a complex formed by the interaction of IXs with other quasiparticles. One plausible origin for the IX complexes under 633 nm on-resonance excitation is the phonon replicas since the energy spacing of 40 meV between IX_{633} and IX_{532} can match well the energy of phonon modes in MoS_2 [57,58]. It is noteworthy that phonon replicas with high emission intensity have been observed in monolayer/bilayer TMDCs [18,44,45,59], benefiting from the enhanced exciton-phonon coupling in the 2D limit [60,61]. In-depth further

experimental and theoretical studies are required to fully understand the detailed microscopic origin of the IX complexes with strong PL intensity under 633 nm on-resonance excitation.

Figure 3(a) presents the circular polarization-resolved PL mapping of bilayer MoS_2 at 10 K under σ^+ (left panel) and σ^- detections (right panel), excited by on-resonance σ^+ light of 633 nm. Two representative cross-cut helicity-resolved PL spectra at $E_z = \pm 0.103 MV/cm$ are shown in Figure 3(b). It is clearly shown that IX complexes under 633 nm excitation feature a strong signal only under the cross-circularly polarized detection, but basically cannot be observed under the co-circularly polarized detection. This evidences that the circular polarization of IX complexes in bilayer MoS_2 can basically reach the theoretical limit (100%) but is negative. This is in stark contrast to the intralayer A excitons whose circular dichroism is small (~ 20%) and positive. The highly unusual close-to-unity, negative circular polarization of IX complexes in bilayer MoS_2 can be understood as the spin-preserving scattering of electron during the exciton formation and strongly suppressed valley depolarization. Upon the 633 nm excitation of σ^+ circularly polarized photon, electron-hole pairs are generated in K valley of upper layer and −K valley of lower layer through spin-conserved intralayer interband transitions, as sketched by the green arrows in Figure 3(c). It is noteworthy that in the light of previous absorption/reflection measurements [30,31,38,62], IXs with considerable optical absorption belong to the species of IX_{532}. Because the energy of IX_{532} is larger than the laser energy (i.e., 1.96 eV), the electron-hole pairs generated via IX transitions can be ignored. The imbalanced distribution of photo-generated carriers between layers within the same valley and between valleys within the same layer would cause relaxation. For instance, the photo-generated electrons in the lower conduction band of −K (K) valley of the lower (upper) layer would relax into the upper conduction band of K valley of the lower layer through valley phonons-assisted intervalley scattering (interlayer tunneling), while the relaxation of photo-generated holes is forbidden [Figure 3(d)], considering that both of these relaxation processes facilitate the spin conservation [18,63,64]. Such spin-preserving scattering of electrons would lead to the formation of σ^- polarized IXs [Figure 3(d)], resulting in the observed negative circular polarization (see Supplemental Material [42] for the details of polarization selection rules).

Based on recent studies [22,65,66], the strong electron-hole exchange interactions dominate the exciton valley depolarization in TMDCs through Maialle-Silva-Sham mechanism. For TMDCs, the valley depolarization rate can be expressed as $\sim \bar{\Omega}^2 \tau$, where $\bar{\Omega}$ is the magnitude of the ensemble-averaged exchange interaction and proportional to the transition dipole, and τ is momentum relaxation time [22]. Owing to the spatially displaced wave functions of electrons and holes, the transition dipole and thus $\bar{\Omega}$ for IX complexes should be several times of magnitude smaller than that for intralayer excitons. As a consequence, Maialle-Silva-Sham valley depolarization mechanism is largely suppressed for IX complexes, resulting in the long valley lifetime and 100% circular polarization.

Apart from the optically addressable valley polarization, the valley degree of freedom of IX complexes can also be controlled by breaking the time-reversal symmetry with an out-of-plane magnetic field [49,67]. Importantly, the enhanced valley Zeeman splitting of IX complexes

compared to intralayer A exciton in bilayer MoS_2 indicate a more effective manipulation of the valley polarization through magnetic fields. Figure 4(a) shows the helicity-resolved magneto-PL spectra under cross-circularly polarized detections at 0T, ±3T and ±8.5T for device D3, excited by 633 nm photons. Note that a small out of plane electric field is applied to drag IX complexes into our detection range. At 0T, σ^+ and σ^- polarized components share the same intensity. When applying a magnetic field, the low-energy components exhibit stronger intensity than the high-energy components, indicating the large formation rate of low-energy IX complexes and the spontaneous circular polarization (Supplemental Material [42]). Figure 4(b) shows the spontaneous circular polarization under different magnetic fields, defined by $\rho = \frac{I(\sigma^+)-I(\sigma^-)}{I(\sigma^+)+I(\sigma^-)}$. The spontaneous valley polarization increases linearly with the magnetic fields: $\rho = \alpha B$, where α indicates the magnetic modulation factor. Through fitting, we extract $\alpha = \sim 7.7\% \cdot T^{-1}$, which, to the best of our knowledge, is the largest value among TMDCs and their heterostructures [26,68-73] [Figure 4(c)]. Such effective manipulation of valley degree of freedom of IX complexes by magnetic field would pave the way for transformative valleytronic devices.

To summarize, we demonstrate the IX complexes with large out-of-plane electric dipole and quantum-confined Stark effec in bilayer MoS_2, under 633 nm on-resonance excitation. The valley degree of freedom of IX complexes in bilayer MoS_2 can be manipulated through both circularly polarized light and magnetic field. Because of the combination of spin-preserving scattering of an electron during the formation and strongly suppressed valley depolarization, IX complexes in bilayer MoS_2 feature a close-to-unity, but negative circular polarization. Moreover, by breaking the valley degeneracy with an out-of-plane magnetic field, we identify a record level of spontaneous valley polarization for IX complexes in bilayer MoS_2. Such highly tunable IX complexes in bilayer MoS_2 with optically and magnetically addressable valley pseudospin hold great promise for the engineering of valley-functional chiral electronic/optoelectronic devices and quantum-computation.

Acknowledgments

We would like to thank Wang Yao in University of Hong Kong for fruitful discussions. This research was supported by the National Key Research and Development Program (Grant Nos. 2020YFA0309600 and 2018YFA0306900), the NSFC (Grants Nos. 61888102, 11834017, and 12074413), the Strategic Priority Research Program of CAS (grant Nos.XDB30000000 and XDB33000000), the Key-Area Research and Development Program of Guangdong Province (Grant No.2020B0101340001), and the Research Program of Beijing Academy of Quantum Information Sciences under Grant No. Y18G11. Z.S. gratefully acknowledges the financial support by Academy of Finland (Grant Nos. 295777, 312297 and 314810), Academy of Finland Flagship Programme (Grant No. 320167, PREIN), the European Union's Horizon 2020 research and innovation program (Grant No. 820423, S2QUIP) and ERC (Grant No. 834742). L.D. gratefully acknowledges the financial support by Academy of Finland (Grant No. 333099). K.W. and T.T. acknowledge support from the Elemental Strategy Initiative conducted by the MEXT,

Japan, Grant Number JPMXP0112101001, JSPS KAKENHI Grant Number JP20H00354 and the CREST(JPMJCR15F3), JST.

Author contributions

G.Z., L.D. and W.Y. supervised this work; L.D. and Y.Z. conceived the project and designed the experiments; Y.Z. fabricated the devices and carried out the optical measurements; S.Y. and Y.Z. performed magneto-PL measurement under the supervision of Y.Y.; K.W. and T.T. contributed high quality *h*-BN crystals; Y.Z., L.D., and W.Y. analyzed the data; L.D., Y.Z., Z.S., W.Y. and G.Z. co-wrote the manuscript. All authors discussed the results and commented on the paper.

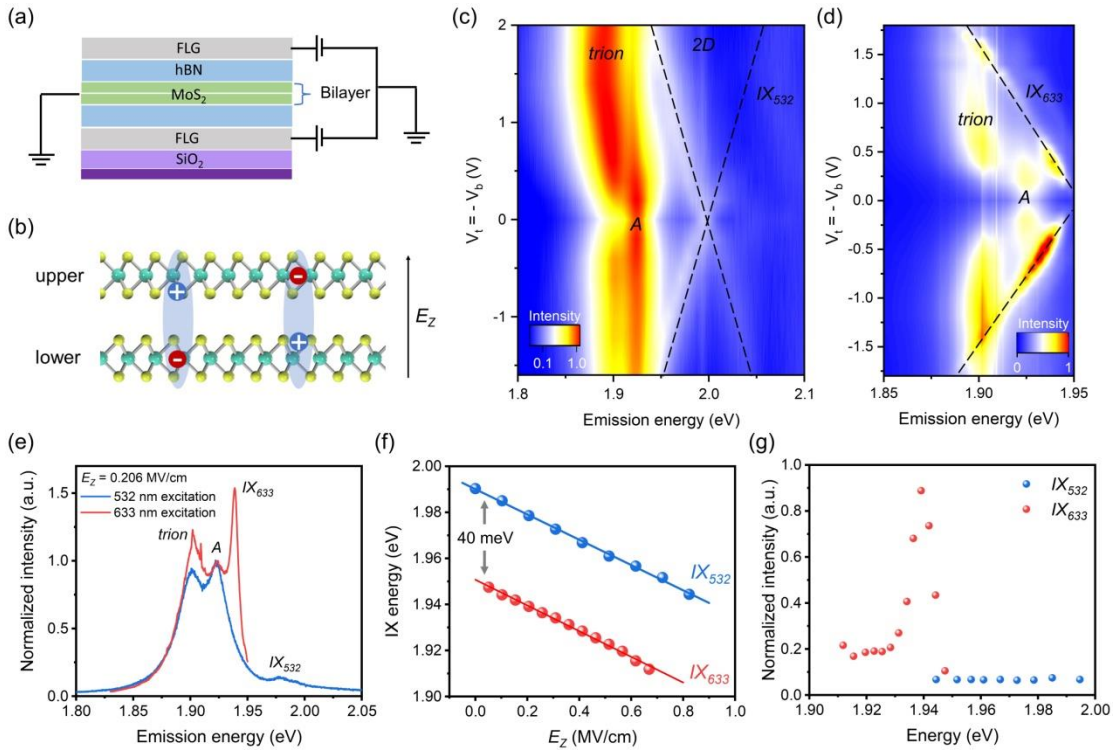


FIG 1. (**a**) Schematic structure of *h*-BN encapsulated dual-gate bilayer MoS_2 device. (**b**) Schematic diagram of the two neutral IXs with electron localized in different layers in bilayer MoS_2. (**c**), (**d**) Color map of PL spectra as a function of the electric field under 532 nm (**c**) and 633 nm excitations (**d**). (**e**) Comparison of PL spectra at a specific electric field under 532 nm and 633 nm excitation, the PL intensity of A is normalized. (**f**) Energies of IX_{532} and IX_{633} as a function of the positive out-of-plane electric field. (**g**) Laser power normalized PL intensity of IX_{532} and IX_{633} as a function of the emission energy.

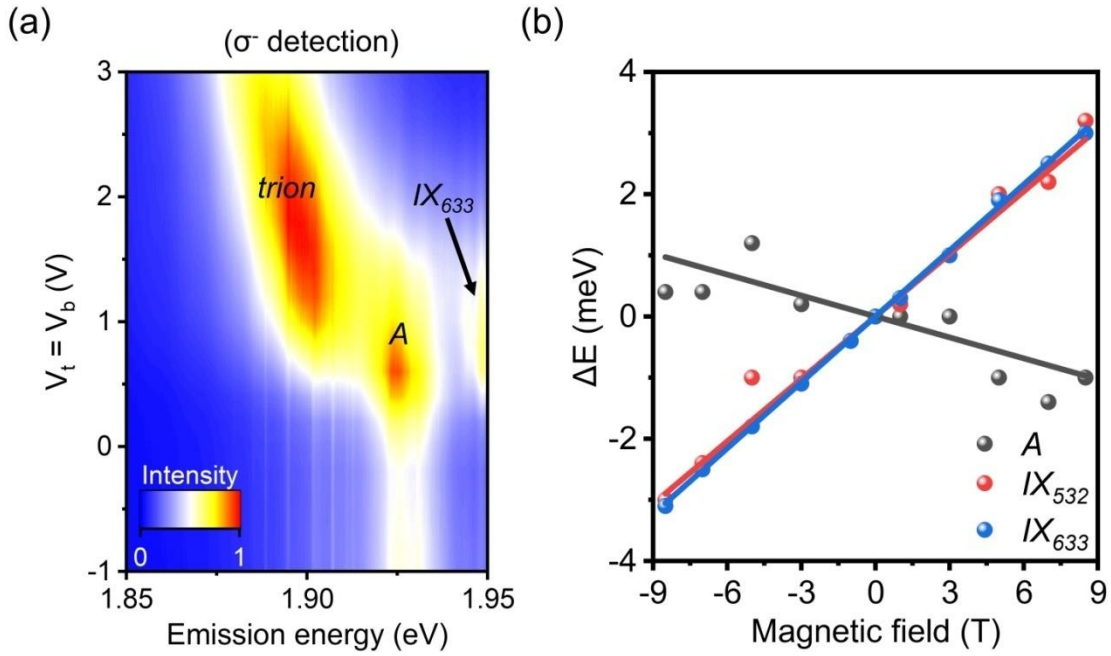


FIG 2. (**a**) Color map of PL spectra as a function of doping density under right-handed (σ^+) excitation at 633 nm, the IX shares the similar evolution with neutral intralayer A exciton. (**b**) Valley Zeeman splitting of IX_{532}, IX_{633} and A exciton under magnetic field.

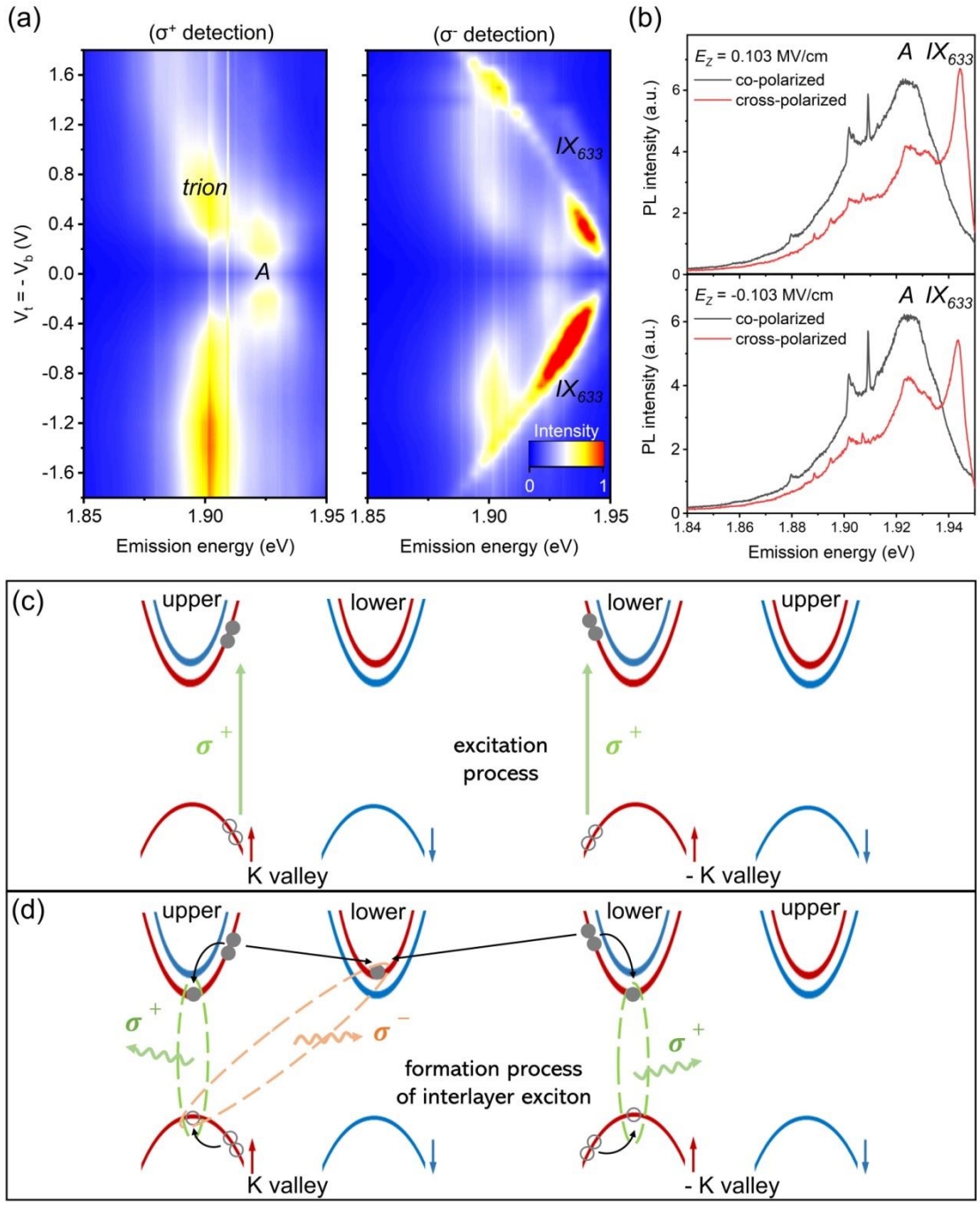


FIG 3. (**a**) Color map of PL spectra as a function of the electric field under co- (left panel) and cross-polarization (right panel) detection. The excitation light is right-handed (σ^+) at 633 nm. (**b**) Cross-cut PL spectra under electric field as the dot black line shown in (**a**). The intensity of IX complexes is basically negligible under co-circularly polarized detection, which indicates a close-to-unity negative circular polarization. (**c**) Helicity-dependent excitation process. (**d**) IXs formation process and helicity-dependent recombination process.

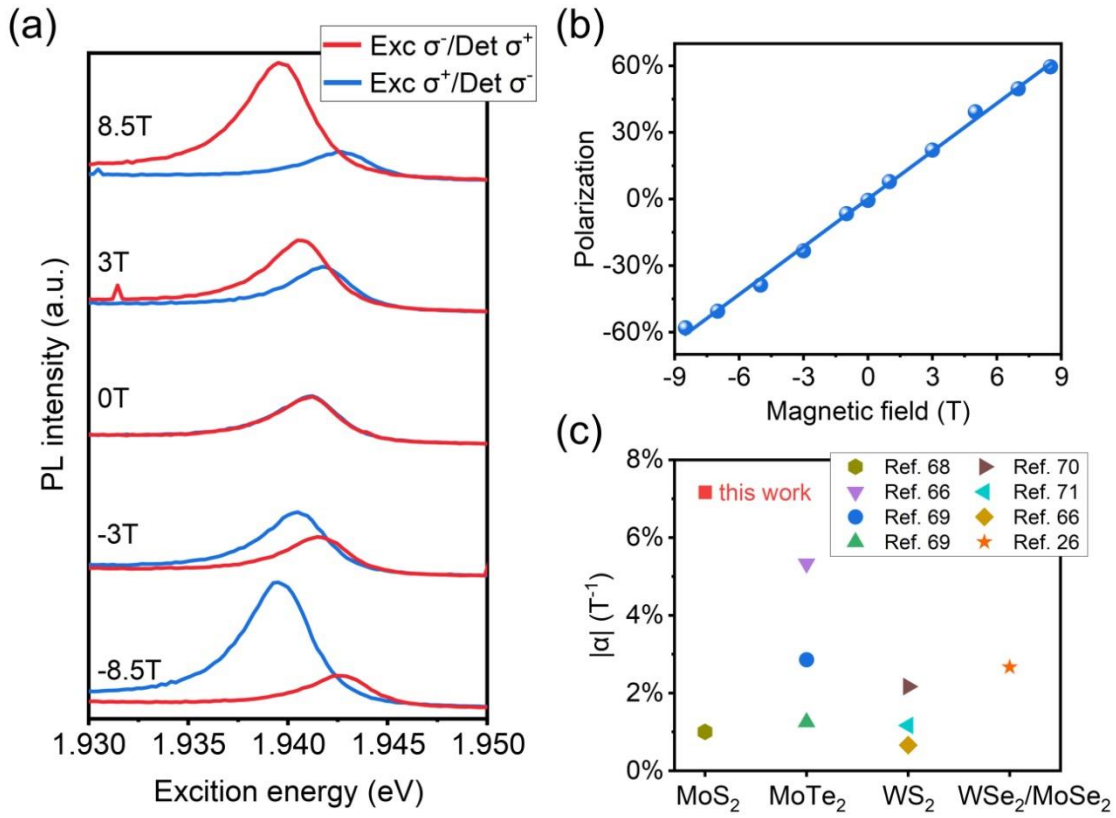


Figure 4. (**a**) PL spectra at specific magnetic field under cross-circularly polarized detection, the excitation energy is 633 nm. (**b**) Spontaneous valley polarization of IX complexes under magnetic field. (**c**) Comparison of magnetic field modulated spontaneous valley polarization between IX complexes in pristine bilayer MoS_2 we detected with excitons in TMDCs and their heterostructures in literature.

[1] G. Wang, A. Chernikov, M. M. Glazov, T. F. Heinz, X. Marie, T. Amand, and B. Urbaszek, Rev. Mod. Phys. **90**, 021001 (2018).

[2] A. Chernikov, T. C. Berkelbach, H. M. Hill, A. Rigosi, Y. Li, O. B. Aslan, D. R. Reichman, M. S. Hybertsen, and T. F. Heinz, Phys. Rev. Lett. **113**, 076802 (2014).

[3] A. Raja, A. Chaves, J. Yu, G. Arefe, H. M. Hill, A. F. Rigosi, T. C. Berkelbach, P. Nagler, C. Schüller, T. Korn *et al.*, Nat. Commun. **8**, 15251 (2017).

[4] K. F. Mak, K. He, C. Lee, G. H. Lee, J. Hone, T. F. Heinz, and J. Shan, Nat. Mater. **12**, 207 (2012).

[5] J. S. Ross, S. Wu, H. Yu, N. J. Ghimire, A. M. Jones, G. Aivazian, J. Yan, D. G. Mandrus, D. Xiao, W. Yao, and X. Xu, Nat. Commun. **4**, 1474 (2013).

[6] G. Plechinger, P. Nagler, A. Arora, R. Schmidt, A. Chernikov, A. G. del Águila, P. C.M. Christianen, R. Bratschitsch, C. Schüller, and T. Korn, Nat. Commun. **7**, 12715 (2016).

[7] E. Courtade, M. Semina, M. Manca, M. M. Glazov, C. Robert, F. Cadiz, G. Wang, T. Taniguchi, K. Watanabe, M. Pierre *et al.*, Phys. Rev. B **96**, 085302 (2017).

[8] E. Liu, J. van Baren, Z. Lu, M. M. Altaiary, T. Taniguchi, K. Watanabe, D. Smirnov, and C. H. Lui, Phys. Rev. Lett. **123**, 027401 (2019).

[9] Y. You, X.-X. Zhang, T. C. Berkelbach, M. S. Hybertsen, D. R. Reichman, and T. F. Heinz, Nat. Phys. **11**, 477 (2015).

[10] Z. Li, T. Wang, Z. Lu, C. Jin, Y. Chen, Y. Meng, Z. Lian, T. Taniguchi, K. Watanabe, S. Zhang, D. Smirnov, and S.-F. Shi, Nat. Commun. **9**, 3719 (2018).

[11] M. Barbone, A. R.-P. Montblanch, D. M. Kara, C. Palacios-Berraquero, A. R. Cadore, D. De Fazio, B. Pingault, E. Mostaani, H. Li, B. Chen *et al.*, Nat. Commun. **9**, 3721 (2018).

[12] S.-Y. Chen, T. Goldstein, T. Taniguchi, K. Watanabe, and J. Yan, Nat. Commun. **9**, 3717 (2018).

[13] Z. Ye, L. Waldecker, E. Y. Ma, D. Rhodes, A. Antony, B. Kim, X.-X. Zhang, M. Deng, Y. Jiang, Z. Lu *et al.*, Nat. Commun. **9**, 3718 (2018).

[14] C. E. Stevens, J. Paul, T. Cox, P. K. Sahoo, H. R. Gutiérrez, V. Turkowski, D. Semenov, S. A. McGill, M. D. Kapetanakis, I. E. Perakis *et al.*, Nat. Commun. **9**, 3720 (2018).

[15] M. Sidler, P. Back, O. Cotlet, A. Srivastava, T. Fink, M. Kroner, E. Demler, and A. Imamoglu, Nat. Phys. **13**, 255 (2017).

[16] K. Wagner, E. Wietek, J. D. Ziegler, M. A. Semina, T. Taniguchi, K. Watanabe, J. Zipfel, M. M. Glazov, and A. Chernikov, Phys. Rev. Lett. **125**, 267401 (2020).

[17] E. Liu, J. van Baren, Z. Lu, T. Taniguchi, K. Watanabe, D. Smirnov, Y.-C. Chang, and C. H. Lui, Nat. Commun. **12**, 6131 (2021).

[18] M. He, P. Rivera, D. V. Tuan, N. P. Wilson, M. Yang, T. Taniguchi, K. Watanabe, J. Yan, D. G. Mandrus, H. Yu *et al.*, Nat. Commun. **11**, 618 (2020).

[19] Z. Li, T. Wang, C. Jin, Z. Lu, Z. Lian, Y. Meng, M. Blei, S. Gao, T. Taniguchi, K. Watanabe *et al.*, Nat. Commun. **10**, 2469 (2019).

[20] E. Liu, J. van Baren, T. Taniguchi, K. Watanabe, Y.-C. Chang, and C. H. Lui, Phys. Rev.

Research **1**, 032007 (2019).
[21] S. Brem, A. Ekman, D. Christiansen, F. Katsch, M. Selig, C. Robert, X. Marie, B. Urbaszek, A. Knorr, and E. Malic, Nano Lett. **20**, 2849 (2020).
[22] P. Rivera, H. Yu, K. L. Seyler, N. P. Wilson, W. Yao, and X. Xu, Nat. Nanotechnol. **13**, 1004 (2018).
[23] K. F. Mak and J. Shan, Nat. Nanotechnol. **13**, 974 (2018).
[24] P. Rivera, K. L. Seyler, H. Yu, J. R. Schaibley, J. Yan, D. G. Mandrus, W. Yao, and X. Xu, Science **351**, 688 (2016).
[25] M. Baranowski, , A. Surrente, L. Klopotowski, J. M. Urban, N. Zhang, D. K. Maude, K. Wiwatowski, S. Mackowski, Y. C. Kung, D. Dumcenco *et al.*, Nano Lett. **17**, 6360 (2017).
[26] P. Nagler, M. V. Ballottin, A. A. Mitioglu, F. Mooshammer, N. Paradiso, C. Strunk, R. Huber, A. Chernikov, P. C. M. Christianen, C. Schüller, and T. Korn, Nature Commun. **8**, 1551 (2017).
[27] Z. Huang, Y. Liu, K. Dini, Q. Tan, Z. Liu, H. Fang, J. Liu, T. Liew, and W. Gao, Nano Lett. **20**, 1345 (2020).
[28] L. A. Jauregui, A. Y. Joe, K. Pistunova, D. S. Wild, A. A. High,Y. Zhou, G. Scuri, K. De Greve, A. Sushko, C.-H. Yu *et al.*, Science **366**, 870 (2019).
[29] A. Ciarrocchi, D. Unuchek, A. Avsar, K. Watanabe, T. Taniguchi, and A. Kis, Nat. Photon. **13**, 131 (2019).
[30] N. Leisgang, S. Shree, I. Paradisanos, L. Sponfeldner, C. Robert, D. Lagarde, A. Balocchi, K. Watanabe, T. Taniguchi, X. Marie *et al.*, Nat. Nanotechnol. **15**, 901 (2020).
[31] N. Peimyoo, T. Deilmann, F. Withers, J. Escolar, D. Nutting, T. Taniguchi, K. Watanabe, A. Taghizadeh, M. F. Craciun, K. S. Thygesen, and S. Russo, Nat. Nanotechnol. **16**, 888 (2021).
[32] A. Arora, M. Drüppel, R. Schmidt, T. Deilmann, R. Schneider, M. R. Molas, P. Marauhn, S. M. de Vasconcellos, M. Potemski, M. Rohlfing, and R. Bratschitsch, Nat. Commun. **8**, 639 (2017).
[33] Y. Shimazaki, I. Schwartz, K. Watanabe, T. Taniguchi, M. Kroner, and A. Imamoğlu, Nature **580**, 472 (2020).
[34] J. Sung, Y. Zhou, G. Scuri, V. Zólyomi, T. I. Andersen, H. Yoo, D. S. Wild, A. Y. Joe, R. J. Gelly, H. Heo *et al.*, Nat. Nanotechnol. **15**, 750 (2020).
[35] F. Carrascoso, D.-Y. Lin, R. Frisenda, and A. Castellanos-Gomez, J. Phys. Mater. **3**, 015003 (2019).
[36] J. Horng, T. Stroucken, L. Zhang, E. Y. Paik, H. Deng, and S. W. Koch, Phys. Rev. B **97**, 241404 (2018).
[37] A. Arora, T. Deilmann, P. Marauhn, M. Drüppel, R. Schneider, M. R. Molas, D. Vaclavkova, S. M. de Vasconcellos, M. Rohlfing, M. Potemski, and R. Bratschitsch, Nanoscale **10**, 15571 (2018).
[38] E. Lorchat, M. Selig, F. Katsch, K. Yumigeta, S. Tongay, A. Knorr, C. Schneider, and S. Höfling, Phys. Rev. Lett. **126**, 037401 (2021).
[39] L. Wang, I. Meric, P. Y. Huang, Q. Gao, Y. Gao, H. Tran, T. Taniguchi, K. Watanabe, L. M. Campos, D. A. Muller *et al.*, Science **342**, 614 (2013).

[40] A. Castellanos-Gomez, M. Buscema, R. Molenaar, V. Singh, L. Janssen, H. S. Van Der Zant, and G. A. Steele, 2D Mater. **1**, 011002 (2014).

[41] Y. Zhao, L. Du, W. Yang, C. Shen, J. Tang, X. Li, Y. Chu, J. Tian, K. Watanabe, T. Taniguchi *et al.*, Phys. Rev. B **102**, 165415 (2020).

[42] See Supplemental Material for details of the device information, interlayer hole hybridization, temperature dependent PL spectra, electrostatic model, doping dependent PL spectra, the polarization selection rules and power dependence of IX complexes, which includes [10-13,41,43,49-53,74-77].

[43] L. Du, M. Liao, G.-B. Liu, Q. Wang, R. Yang, D. Shi, Y. Yao, and G. Zhang, Phys. Rev. B **99**, 195415 (2019).

[44] Z. Wang, Y.-H. Chiu, K. Honz, K. F. Mak, and J. Shan, Nano Lett. **18**, 137 (2018).

[45] M. M. Altaiary, E. Liu, C.-T. Liang, F.-C. Hsiao, J. van Baren, T. Taniguchi, K. Watanabe, N. M. Gabor, Y.-C. Chang, and C. H. Lui, preprint arXiv:2101.11161 (2021).

[46] C. Jin, J. Kim, K. Wu, B. Chen, E. S. Barnard, J. Suh, Z. Shi, S. G. Drapcho, J. Wu, P. J. Schuck, S. Tongay, and F. Wang, Adv. Fun. Mater. **27**, 1601741 (2017).

[47] D. Kozawa, R. Kumar, A. Carvalho, K. K. Amara, W. Zhao, S. Wang, M. Toh, R. M. Ribeiro, A. H. Castro Neto, K. Matsuda, and G. Eda, Nat. Commun. **5**, 4543 (2014).

[48] K. Okamoto, I. Niki, A. Shvartser, Y. Narukawa, T. Mukai, and A. Scherer, Nat. Mater. **3**, 601 (2004).

[49] G. Aivazian, Z. Gong, A. M. Jones, R.-L. Chu, J. Yan, D. G. Mandrus, C. Zhang, D. Cobden, W. Yao, and X. Xu, Nat. Phys. **11**, 148 (2015).

[50] A. Srivastava, M. Sidler, A. V. Allain, D. S. Lembke, A. Kis, and A. Imamoğlu, Nat. Phys. **11**, 141 (2015).

[51] Y. Li, J. Ludwig, T. Low, A. Chernikov, X. Cui, G. Arefe, Y. D. Kim, A. M. van der Zande, A. Rigosi, H. M. Hill, *et al.*, Phys. Rev. Lett. **113**, 266804 (2014).

[52] D. MacNeill, C. Heikes, K. F. Mak, Z. Anderson, A. Kormányos, V. Zólyomi, J. Park, and D. C. Ralph, Phys. Rev. Lett. **114**, 037401 (2015).

[53] H. Yu, G.-B. Liu, and W. Yao, 2D Mater. **5**, 035021 (2018).

[54] K. L. Seyler, P. Rivera, H. Yu, N. P. Wilson, E. L. Ray, D. G. Mandrus, J. Yan, W. Yao, and X. Xu, Nature **567**, 66 (2019).

[55] M. Brotons-Gisbert, H. Baek, A. Molina-Sánchez, A. Campbell, E. Scerri, D. White, K. Watanabe, T. Taniguchi, C. Bonato, and B. D. Gerardot Nat. Mater. **19**, 630 (2020).

[56] A. Y. Joe, L. A. Jauregui, K. Pistunova, A. M. Mier Valdivia, Z. Lu, D. S. Wild, G. Scuri, K. De Greve, R. J. Gelly, Y. Zhou *et al.*, Phys. Rev. B **103**, L161411 (2021).

[57] L. Zhang and Q. Niu, Phys. Rev. Lett. **115**, 115502 (2015).

[58] H. Dery and Y. Song, Phys. Rev. B **92**, 125431 (2015).

[59] Z. Huang, Y. Zhao, T. Bo, Y. Chu, J. Tian, L. Liu, Y. Yuan, F. Wu, J. Zhao, L. Xian *et al.*, preprint arXiv:2108.09129 (2021).

[60] L. Du, M. Liao, J. Tang, Q. Zhang, H. Yu, R. Yang, K. Watanabe, T. Taniguchi, D. Shi, Q.

Zhang, and G. Zhang, Phys. Rev. B **97**, 235145 (2018).

[61] A. Raja, M. Selig, G. Berghäuser, J. Yu, H. M. Hill, A. F. Rigosi, L. E. Brus, A. Knorr, T. F. Heinz, E. Malic, and A. Chernikov, Nano Lett. **18**, 6135 (2018).

[62] I. C. Gerber, E. Courtade, S. Shree, C. Robert, T. Taniguchi, K. Watanabe, A. Balocchi, P. Renucci, D. Lagarde, X. Marie, and B. Urbaszek, Phys. Rev. B **99**, 035443 (2019).

[63] R. Pisoni, T. Davatz, K. Watanabe, T. Taniguchi, T. Ihn, and K. Ensslin, Phys. Rev. Lett. **123**, 117702 (2019).

[64] J. R. Schaibley, P. Rivera, H. Yu, K. L. Seyler, J. Yan, D. G. Mandrus, T. Taniguchi, K. Watanabe, W. Yao, and X. Xu, Nat. Commun. **7**, 13747 (2016).

[65] C. Zhu, K. Zhang, M. Glazov, B. Urbaszek, T. Amand, Z. Ji, B. Liu, and X. Marie, Phys. Rev. B **90**, 161302 (2014).

[66] K. Hao, G. Moody, F. Wu, C. K. Dass, L. Xu, C.-H. Chen, L. Sun, M.-Y. Li, L.-J. Li, A. H. MacDonald, and X. Li, Nature Physics **12**, 677 (2016).

[67] L. Du, T. Hasan, A. Castellanos-Gomez, G.-B. Liu, Y. Yao, C. N. Lau, and Z. Sun, Nat. Rev. Phys. **3**, 193 (2021).

[68]C. Jiang, F. Liu, J. Cuadra, Z. Huang, K. Li, A. Rasmita, A. Srivastava, Z. Liu, and W.-B. Gao, Nat. Commun. **8**, 802 (2017).

[69] G. Wang, L. Bouet, M. Glazov, T. Amand, E. Ivchenko, E. Palleau, X. Marie, and B. Urbaszek, 2D Mater. **2**, 034002 (2015).

[70] F. Cadiz, E. Courtade, C. Robert, G. Wang, Y. Shen, H. Cai, T. Taniguchi, K. Watanabe, H. Carrere, D. Lagarde *et al.*, Phys. Rev. X **7**, 021026 (2017).

[71] A. Arora, R. Schmidt, R. Schneider, M. R. Molas, I. Breslavetz, M. Potemski, and R. Bratschitsch, Nano Lett. **16**, 3624 (2016).

[72] P. Nagler, M. V. Ballottin, A. A. Mitioglu, M. V. Durnev, T. Taniguchi, K. Watanabe, A. Chernikov, C. Schüller, M. M. Glazov, P. C. M. Christianen, and T. Korn, Phys. Rev. Lett. **121**, 057402 (2018).

[73] G. Plechinger, P. Nagler, . Arora, A. G. del Águila, M. V. Ballottin, T. Frank, P. Steinleitner, M. Gmitra, J. Fabian, P. C. M. Christianen *et al.*, Nano Lett. **16**, 7899 (2016).

[74] Z. Gong, G.-B. Liu, H. Yu, D. Xiao, X. Cui, X. Xu, and W. Yao, Nat. Commun. **4**, 2053 (2013).

[75] G.-B. Liu, D. Xiao, Y. Yao, X. Xu, and W. Yao, Chem. Soc. Rev. **44**, 2643 (2015).

[76] H. Yu, G. B. Liu, P. Gong, X. Xu, and W. Yao, Nat. Commun. **5**, 3876 (2014).

[77] J. Zhang, L. Du, S. Feng, R.-W. Zhang, B. Cao, C. Zou, Y. Chen, M. Liao, B. Zhang, S. A. Yang, G. Zhang, and T. Yu, Nat. Commun. **10**, 4226 (2019).